



ELSEVIER

Angular, energy, and population distributions of neutral atoms desorbed by keV ion beam bombardment of Ni{001}

Chun He ^{*}, S.W. Rosencrance, Z. Postawa ¹, C. Xu, R. Chatterjee, D.E. Riederer, B.J. Garrison, N. Winograd

Department of Chemistry, The Pennsylvania State University, University Park, PA 16802, USA

Abstract

Multi-photon resonance ionization, time-of-flight mass spectrometry and imaging techniques have been employed to measure the polar-angle, kinetic energy, and population distributions of Ni atoms desorbed from 5 keV Ar ion bombarded Ni{001}. The measured angle- and energy-resolved intensity maps of the sputtering yield provide a set of data that can be used to examine the detailed interactions between the particles of the solid surface during the sputtering event. The results show a considerable degree of anisotropy associated with both the ejection angle as well as the crystallographic direction. In order to have an understanding of the interactions of the desorbed particles with the surface, molecular dynamics simulations of the ion-induced sputtering event are performed. The agreement between experimental and computer simulation results is excellent. Measurements performed on excited states of sputtered Ni show that the valence electron shell structure is an important factor in determining the angle-integrated kinetic energy distribution while the magnitude of the excitation energy is of secondary importance. Population distribution among different electronic states is obtained through two sets of measurements performed on different instruments. Both measurements employ the same resonant ionization schemes and laser fluences. The results show that the a^3D_3 and a^3D_2 states are more heavily populated than is predicted by a Boltzmann-type distribution.

1. Introduction

Energetic ion impact on a solid initiates a complex dynamical chain of events which include atomic motion, electronic excitation, ionization, and desorption of atomic and molecular species. Measurements on the desorbed particles during the ion–solid interaction process provide a valuable opportunity to examine this complex many-body interaction system [1]. Numerous experiments have been performed by different means to measure various parameters, such as yield, kinetic energy and charged fraction of the ejected particles [2–4]. Since an appreciable portion of the ejected particles are populated in electronic excited states, measurement of the above quantities as a function of each state should provide information about the excitation and de-excitation processes [5–8]. However, after more than two decades of research, many fundamental questions have not yet been answered. This is due to both the extreme complexity of the events which result from

keV ion bombardment and the lack of detailed and reliable experimental data. The situation has been greatly improved with the development of new experimental techniques. Doppler-shifted laser-induced fluorescence (DSLIF) spectroscopy [2,5,9–11] and energy- and angle-resolved neutral (EARN) spectrometry [6–8,12–14] are capable of obtaining state-resolved kinetic energy distribution.

We report experiments on Ni atoms ejected from a Ni{001} single crystal due to 5 keV Ar ion bombardment. The measurements are state-selected, kinetic energy and angle-resolved. In order to fully understand the anisotropic spatial distributions of the ejected Ni atoms from the Ni{001}, a molecular dynamics (MD) computer simulation has been performed on a model single crystal. This simulation employs a MD/MC-CEM interaction potential to describe the forces between Ni atoms during the collision cascade [15]. Experiments were performed on the excited, metastable states of Ni. The ejected Ni atoms are selectively ionized from fine structure states a^3F_j and a^3D_j which have valence electron configurations of $3d^84s^2$ and $3d^94s^1$, respectively. Angular distributions of excited state Ni atoms show basically the same angular anisotropy regardless of excitation energy and electron configuration,

^{*} Corresponding author.

¹ Permanent address: Institute of Physics, Jagellonian University, 30-059 Krakow, ul. Reymonta 4, Poland.

indicating the interactions between nuclei and the solid crystal are mainly responsible for the observed angular anisotropy. However there is a clear evidence that valence electron shell structure is an important factor in determining the angle-integrated kinetic energy distribution while the magnitude of the excitation energy seems to be less significant.

A few years ago, Craig et al. proposed an orbital deexcitation model to account for the lack of $a^2P_{3/2}$ excited state in atoms sputtered from an In foil [16]. The model suggests that the factors which are important in determining whether an atom in an excited state will relax as it departs from the surface depend on the electronic character of its fine-structure states. When the s-orbital is filled, the s-electrons can effectively shield the d-electrons from interaction with the metal, therefore, relaxation processes are minimal and the velocity distribution of the excited atoms is independent of atomic state. On the other hand, when the d-electrons are not completely being shielded or are exposed, the atoms are partially or completely deexcited to the ground state.

The present study shows conclusive experimental evidence that electronic structure rather than the excitation energy is the primary factor in determining kinetic energy distributions of sputtered neutral species. Nickel atoms ionized from the closed s-shell states a^3F_4 , and a^3F_3 show a general profile predicted by an analytical model [17]. Nickel atoms ionized from the open s-shell states a^3D_3 and a^3D_2 show a distinctly different distribution.

The population distribution among different electronic states is obtained through two sets of measurements performed on two experiment instruments: one which measures the energy- and angle-integrated resonance ionization signal intensities of the sputtered Ni; and the other which measures the resonance ionization signal intensities of thermally evaporated Ni atoms with a known temperature. Both measurements employ the same resonant ionization schemes and laser fluences. The results show that the population distribution is distinct from a Boltzmann-type distribution with the a^3D_3 and a^3D_2 states heavily populated.

2. Experimental

The experimental setup and measurement of energy-, and angle-resolved neutrals (EARN) have been described in detail previously [8,12]. The population distribution among different electronic states is obtained by combining data measured on the EARN apparatus and data measured on a high vacuum cell capable of producing gas phase Ni atoms through thermal evaporation. Laser-power-dependence studies have been performed for each of the involved transitions on both experiments. In all cases the photoion signals show a linear dependence on the laser power from 50 to 300 MW/cm².

3. Results and discussion

3.1. Energy-resolved angular distribution of sputtered Ni atoms

The experimentally obtained EARN distributions of Ni atoms in the ground electronic state are shown in Fig. 1. There is considerable anisotropy associated with both the polar-angle distribution as well as the crystallographic directions. This behavior was also reported for Rh(001) and explained on the basis of MD computer simulations of the ion bombardment event [18]. It was concluded that these angular anisotropies result from the specific geometrical structure of the top surface layers of the single crystal. It was shown that the polar-angle distribution is mainly determined by the relative position of surface atoms which influence the trajectories of exiting atoms via channelling and blocking mechanisms.

We performed MD computer simulations for 3 keV Ar ions impacting at normal incidence on a Ni(001) model crystal composed of 9 layers with 200 atoms per layer. The potential function used in the present simulation is the MD/MC-CEM potential [15]. The MD/MC-CEM potential has been chosen in this study since recent studies

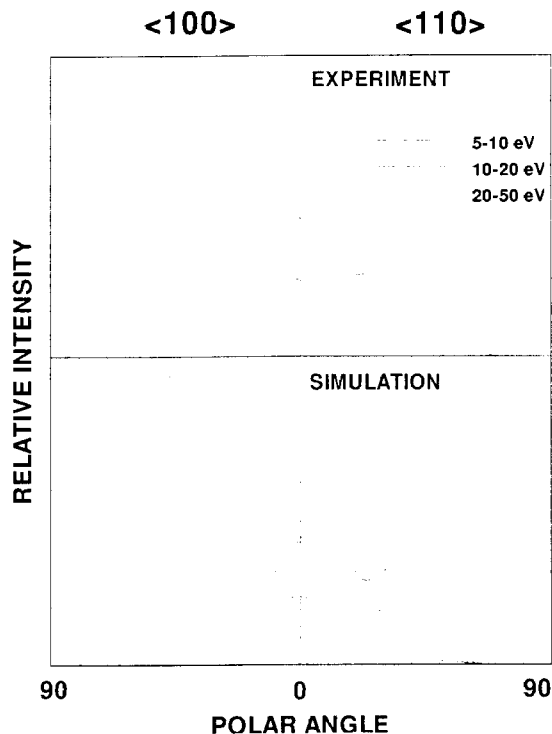


Fig. 1. Energy-resolved polar angle distributions of sputtered Ni atoms in the ground state along $\langle 100 \rangle$ and $\langle 110 \rangle$ azimuthal directions. The top graphs are measured experimentally and the bottom graphs are obtained by integrating 1200 trajectories from the molecular dynamics computer simulations.

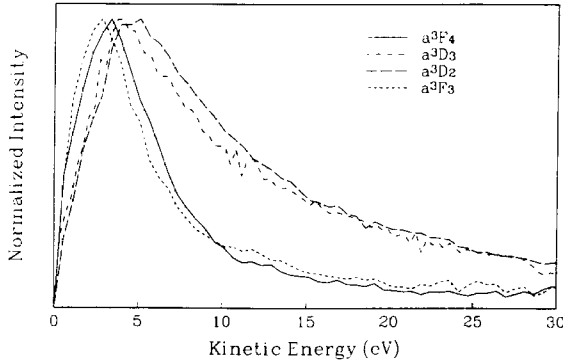


Fig. 2. Angle-integrated kinetic energy distributions of the measured Ni atoms in the four metastable states which belong to the closed s-shell structure, a^3F_4 (ground state) and a^3F_3 (third-excited state, 0.165 eV), and to the open d-shell structure, a^3D_3 , (first-excited state, 0.025 eV) and a^3D_2 , (second-excited state, 0.109 eV), for the $\langle 100 \rangle$ azimuthal direction.

suggest it more accurately reflects the surface binding energy [15].

Results of the MD simulations are presented in the bottom part of Fig. 1. Note that all of the important features of the experimental data are well-reproduced by the calculation. The success of the present simulation demonstrates the validity of applying the MD/MC-CEM potential to accurately describe the energetic ion-solid interaction event. The MD simulation can reveal more information which cannot be accessed experimentally. For example, it shows that 86% of the total ejected atoms originate from the first layer of the crystal, and 12% from the second layer. The remaining 2% of the total yield arises from third and deeper layers.

3.2. Influence of the valence shell electron configuration

The kinetic energy distributions of the measured Ni atoms in the metastable, open s-shell states a^3D_3 , and a^3D_2 , and closed s-shell states a^3F_4 , and a^3F_3 , are presented in Fig. 2 for the $\langle 100 \rangle$ azimuthal direction. From these plots it is evident that the velocity distributions of Ni atoms from different electronic states with different excitation energies but the same electronic shell structure look similar. Velocity distributions of Ni atoms with different electron-shell structures are remarkably different, even when they have almost similar excitation energies. The kinetic energy distributions along the $\langle 110 \rangle$ azimuth show the same character as those along the $\langle 100 \rangle$ direction.

There are two important, and quite different features between these two groups of states. First, the velocity distributions from a closed s-shell are all peaked at the same value of 3.2 eV, which is about 1 eV smaller than those from the open s-shell structure, all of which are peaked at 4.4 eV. In the language of Thompson [19], the open s-shell states have a larger effective ‘surface binding energy’. The result is consistent with the electron shell

structure model discussed in the introduction. These atoms are effectively shielded by the filled s-orbital and do not interact as strongly with the metal electrons while departing from the surface. That is, the effective surface binding energy is smaller for atoms having a closed outer shell orbital and is larger for atoms having an open outer shell orbital. Secondly, the atoms ejected from states of open s-shell configuration have broader kinetic energy distributions than those from states of closed s-shell configuration. As these plots are all normalized to their peak intensities, and the ejected particles of high kinetic energy are less likely to be influenced from the interaction with the surface, this observation implies excited Ni atoms with an open s-shell electron configuration are more likely to de-excite than atoms with a closed s-shell configuration.

3.3. Population partitioning among different electronic states

The interpretation of the relationship between the number density of sputtered atoms and the one-color MPRI photoion signal has been a long standing issue [20]. Although there are many studies, both theoretically and spectroscopically devoted to this field, an unambiguous population distribution can not be obtained from the measured photo-ion signal. This is largely due to the complex spectroscopic structure of an atom above its ionization limit [20]. In the present study a new approach is adopted to overcome this obstacle. The solution is to perform another experiment with the same MPRI scheme which has a known population distribution among different states. For example, a Boltzmann distribution for thermally excited particles.

For an initial state i , the MPRI signal via an intermediate state u can be expressed as

$$I_{iu}^S = N_i^S \Phi_{iu}(g_i, g_u, f_{iu}, A_u, \sigma_u, P) \eta^S, \quad (1)$$

$$I_{iu}^T = N_i^T \Phi_{iu}(g_i, g_u, f_{iu}, A_u, \sigma_u, P) \eta^T, \quad (2)$$

where, with superscript ‘‘S’’ representing quantities measured in the sputtering experiment and ‘‘T’’ representing thermal evaporation experiment, I_{iu} is signal intensity, N_i is the population, and η is the detection efficiency. Φ_{iu} is a function which depends on the laser fluence P ; the degeneracies of initial state i and intermediate state u , g_i and g_u , respectively; the oscillator strength of transition $i \rightarrow u$, f_{iu} ; and the lifetime, A_u , and ionization cross section, σ_u , of state u . In most of the cases Φ_{iu} is unknown.

For initial states i and j ionized via a single upper state u , we have

$$N_i^S/N_j^S = N_i^T/N_j^T \{I_{iu}^S/I_{ju}^S\} \{I_{ju}^T/I_{iu}^T\}. \quad (3)$$

Therefore, the relative population of the sputtered Ni at different electronic states can be obtained from the known population in the thermal evaporation experiment, assuming that it exhibits a Boltzmann distribution.

Table 1
Relative population of sputtered Ni in different electronic states

Ni atom initial state	Energy [eV]	Popul. dist. sputtering	Boltzmann dist. at 956°C
a^3F_4	0	1	1
a^3D_3	0.025	5.71	0.79
a^3D_2	0.109	7.42	0.36
a^3F_3	0.165	0.96	0.21

The relative population of the sputtered Ni atoms at different states are listed in Table 1, along with a calculated Boltzmann distribution at the temperature of Ni in the thermal evaporation experiment. The most striking feature is the non-Boltzmann-type distribution observed in the sputtering experiment with the a^3D_3 and a^3D_2 states more heavily populated than the ground state a^3F_4 . Although discrepancies from the Boltzmann-type distribution have been observed by several research groups [5,8,21], this is the first time population inversions in the sputtered particles have been observed. At present we do not understand the mechanisms which cause preferential population of these two states.

4. Conclusion

State-selected, angle- and energy-resolved intensity distributions of Ni atoms desorbed from a 5 keV Ar ion bombarded Ni(001) surface have been measured. The energy-resolved angular distributions show a considerable degree of anisotropy associated with both the polar ejection angle and the crystallographic direction. These intensity distribution anisotropies are reproduced by a molecular dynamics computer simulation, which emulates the energetic ion-solid interaction event, with remarkable resemblance.

Experiments performed on the excited states of sputtered Ni atoms reveal very interesting results which may lead to further understanding of excitation and deexcitation mechanisms during the ion-solid interaction event. Angular distributions of excited state Ni atoms show basically the same angular anisotropy regardless of their excitation energy and electron configuration, indicating the interactions between nuclei and the solid crystal are mainly responsible for the observed angular anisotropy. However there is evidence that valence electron shell structure is the dominant factor in determine the angle-integrated kinetic energy distribution while the potential energy effect is less important. The population of the sputtered Ni atoms in different states is found not to obey the Boltzmann distribution with

a^3D_3 and a^3D_2 states more heavily populated than the ground state.

Acknowledgements

The authors appreciate the financial support from the Department of Energy, the Office of Naval Research, the National Science Foundation and the M. Sklodowska-Curie Fund MEN/NSF-93-144. The authors thank Drs. W. Ernst, D. Shirley and D. Sanders for useful discussions about this work.

References

- [1] N. Winograd, Prog. Solid State Chem. 13, (1982) 285.
- [2] G. Betz, Nucl. Instr. and Meth. B 27 (1987) 104, and references cited therein.
- [3] W.O. Hofer, Topics Appl. Phys. 64 (1991) 15.
- [4] M.L. Yu, Topics Appl. Phys. 64 (1991) 91.
- [5] M.L. Yu, D. Grischkowsky and A.C. Balant, Phys. Rev. Lett. 48 (1982) 427.
- [6] M. El-Maazawi, R. Maboudian, Z. Postawa and N. Winograd, Phys. Rev. B 43 (1991) 12078.
- [7] N. Winograd, M. El-Maazawi, R. Maboudian, Z. Postawa, D.N. Bernardo and B.J. Garrison, J. Chem. Phys. 96 (1992) 6314.
- [8] Chun He, Z. Postawa, M. El-Maazawi, S. Rosencrance, B.J. Garrison and N. Winograd, J. Chem. Phys. 101 (1994) 6226.
- [9] B. Schweer and H.L. Bay, Appl. Phys. A 29 (1982) 53.
- [10] C.E. Young, M.F. Calaway, M.J. Pellin and D.M. Gruen, J. Vac. Sci. Technol. A 2 (1984) 693, and references cited therein.
- [11] E. Dullini, Appl. Phys. A 38 (1985) 131.
- [12] P.H. Kobrin, G.A. Schick, J.P. Baxter and N. Winograd, Rev. Sci. Instr. 57 (1986) 1354.
- [13] N. Winograd, M. El-Maazawi, R. Maboudian, Z. Postawa, D.N. Bernardo and B.J. Garrison, J. Chem. Phys. 96 (1992) 3846.
- [14] D.N. Bernardo, M. El-Maazawi, R. Maboudian, Z. Postawa, N. Winograd and B.J. Garrison, J. Chem. Phys. 97 (1992) 3846.
- [15] T.J. Racker and A.E. DePristo, Int. Rev. Phys. Chem. 10 (1991) 1, and references cited therein.
- [16] B.I. Craig, J.P. Baxter, J. Singh, G.A. Schick, P.H. Kobrin, B.J. Garrison and N. Winograd, Phys. Rev. Lett. 57 (1986) 1351.
- [17] R. Kelly, Phys. Rev. B 25 (1982) 700.
- [18] R. Maboudian, Z. Postawa, M. El-Maazawi, B.J. Garrison and N. Winograd, Phys. Rev. B 42 (1990) 7311.
- [19] M.W. Thompson, Philos. Mag. 18 (1968) 377.
- [20] see, for example, G.S. Hurst, M.G. Payne, S.D. Kramer and J.P. Young, Rev. Mod. Phys. 51 (1979) 767.
- [21] T.J. Whitaker, Anjun Li, P.L. Jones and R.O. Watts, J. Chem. Phys. 98 (1993) 5887.